Evidence for Elastoplasticity in Dissipative Heavy-Ion Collisions

M. Rhein,[1] R. Barth,[1] E. Ditzel,[1] H. Feldmeier,[2] E. Kankeleit,[1] V. Lips,[1] C. Müntz,[1] W. Nörenberg,[1,2] H. Oeschler,[1] A. Piechaczek,[1] W. Polai,[1] and I. Schall[1]

[1]*Institut für Kernphysik, Technische Hochschule, D-6100 Darmstadt, Germany*

[2]*Gesellschaft für Schwerionenforschung, D-6100 Darmstadt, Germany*

(Received 13 April 1992)

From the measured yield of δ electrons with energies between 3 and 8 MeV, emitted in the heavy-ion reaction Pb+Pb at 12 MeV/nucleon incident energy, a very fast deceleration of the nuclei in the approach phase is inferred which is much faster than predicted by the microscopic one-body dissipation model. Since the deceleration time is smaller than or comparable to the thermal equilibration time, the dissipation process is non-Markovian and therefore memory effects have to be included. This is performed on the basis of dissipative diabatic dynamics, which describes elastoplastic properties. The new diabatic one-body dissipation model reproduces the fast deceleration and the long nuclear contact time.

PACS numbers: 25.70.Lm

In the past decade it has been demonstrated that δ-electron spectroscopy serves as a method to determine the time evolution of dissipative heavy-ion collisions. The dependence of the lepton spectra on the nuclear trajectories was discussed in Refs. [1,2] and is best illustrated when using the scaling model [2]. In this model the transition amplitude a_{if} of a bound electron to be excited into the continuum is given by the Fourier transform

$$a_{if} \propto \frac{1}{E_{if}} \int_{-\infty}^{\infty} dt \frac{\dot{R}(t)}{R(t)} \exp\left[i \frac{E_{if}}{\hbar} t \right], \tag{1}$$

where E_{if} is the difference between the initial and final energies of the electron. The quantity $R(t)$ denotes twice the time-dependent root-mean-square radius of the charge distribution of the two nuclei [3]. The ratio $\dot{R}(t)/R(t)$ contains the information about the trajectory. The spectral shapes calculated within the scaling model are in good agreement with the more elaborate coupled channel calculations [4] which are used in the following analysis.

The shape of the δ-electron spectra is mainly determined by two features of the trajectories. One is the interplay of conservative and frictional forces during the separation of the nuclei, which causes a time delay compared to Coulomb trajectories and leads to a steeper decrease of the spectra for electron energies below 2 MeV. This has been shown in several experiments [5–8]. The other feature is the fast deceleration of the nuclei at the beginning of the collision, which leads to a rapid change of $\dot{R}/R$ and thus to the emission of high-energy δ electrons [9]. So far these electrons have only been measured up to 3.5 MeV. To obtain sufficient yield in the high-energy part of the δ-electron spectra, large relative velocities of the nuclei are needed when the deceleration due to nuclear forces sets in. Therefore, we performed an experiment at 12.0 MeV/nucleon bombarding energy for the collision system Pb+Pb and measured the electron energy spectra up to 8 MeV.

The experiment was carried out with the TORI spectrometer [10], installed at the UNILAC accelerator of GSI Darmstadt. About 10^9 ions of ^{208}Pb per second were impinging on ^{12}C-backed ^{208}Pb targets of ≈ 350 μg/cm^2 thickness. The TORI spectrometer is a magnetic transport system designed to measure simultaneously electrons and positrons in coincidence with the scattered heavy ions. To extend the energy range of electrons up to 8 MeV, a new detector [11] is placed in the solenoidal field of the TORI spectrometer. The energy of the electrons is measured with a 5-cm-long plastic cylinder (NE102) of 7.5 cm diameter. The rather poor energy resolution of $\Delta E/E \approx 10\%$ for energies above 2.0 MeV is tolerated in order to have the advantage of a good time resolution ($\Delta t \approx 1$ ns). To separate electrons from γ rays and neutrons, a silicon surface barrier ΔE detector of 500 μm thickness is placed in front of the plastic block. As a result of its very low detection efficiency for gamma rays and neutrons this counter is used as a trigger for electrons. Furthermore, we profit from the high electron transport efficiency to the detector in the solenoidal field. This yields a solid-angle ratio of 122 for electrons compared to γ rays and neutrons. The additional suppression obtained by the ΔE counter results in a detection-efficiency ratio of $\varepsilon_{e^-}/\varepsilon_\gamma \approx 4500$. A cylindrical aluminum baffle mounted in front of the detector provides a good suppression of the very high yield of low-energy electrons which spiral close to the magnetic axis. With an additional time-of-flight analysis a complete suppression of neutron events is obtained. The response function is determined by using high-energetic electrons delivered by an electron accelerator [11] and by the β source ^{106}Ru.

The other counters are similar to those used in previous experiments [8]. Si(Li) counters detect electrons and positrons in the energy range of 0.8 MeV $\leq E_{e^-} \leq$ 2.5 MeV. A pair of position-sensitive heavy-ion counters is used to study kinematical coincidences by measuring the angles of the outgoing fragments and to distinguish sequential fission events from scattered heavy ions. These parallel-plate avalanche detectors work with a delay-line technique. The delay lines are read out on both sides in order to recognize double-hit events. They originate from cases where one reaction partner undergoes fission. The

total kinetic-energy loss (TKEL) of the collisions is calculated from the scattering angles of the heavy ions with a resolution of about 50% due to angular resolution and neutron evaporation.

For high TKEL values a significant amount of the measured electrons originate from nuclear processes. These contributions have to be subtracted because only the atomic part of the spectra contains the information about the nuclear trajectories. To determine the contribution of leptons from nuclear origin, the γ-ray spectra are measured with a 10 cm×15 cm BaF_2 crystal. The γ detector is mounted perpendicular to the beam axis, leading to maximum Doppler broadening without a significant mean Doppler shift. As for the plastic detector, the good time resolution of the BaF_2 crystal is necessary to separate γ rays from neutron-induced background events. For the conversion of the measured γ spectra into lepton spectra theoretical conversion coefficients have been used [12,13]. The validity of the multipolarity decomposition of the γ spectra is controlled by the comparison of measured and converted positron spectra. This procedure is very accurate for high TKEL values where only a small fraction of positrons ($\lesssim 10\%$) originate from atomic processes. The conversion-electron background amounts to less than 10% of the measured electron spectra.

To compare the measured δ-electron spectra with theoretical predictions, the impact parameter distributions have to be known. This is achieved with a Monte Carlo simulation [8] using the deflection functions calculated with the trajectory models discussed below. Applying the same cuts in the simulated and measured TKEL versus scattering-angle correlations we obtain the impact-parameter distributions for the selected event class.

In Fig. 1 the δ-electron spectra which have been measured in coincidence with Pb+Pb collisions are shown. With increasing TKEL the spectra exhibit a steeper descent in the region up to 2.0 MeV and an increasing yield of high-energy δ electrons compared to calculations based on Rutherford trajectories (dotted lines). The lines in Fig. 1 are the results obtained with coupled-channel calculations [14] where only $R(t)$ enters for the trajectories. All theoretical spectra are multiplied by a factor of 1.5 in order to match the absolute height in the spectrum for elastic collisions.

For the description of the nuclear trajectories we start out from the microscopic semiclassical one-body dissipation model as explained in detail in Ref. [15]. Without adjustable parameters this model describes a large body of experimental data on nucleus-nucleus collisions [16]. Its friction coefficients are calculated microscopically, based on the ideas of the window and wall dissipation [17]. In particular, for the system Pb+Pb at an incident energy of 8.6 MeV/nucleon [8], the δ-electron spectra up to 2 MeV are well accounted for within the one-body dissipation model. The observed long contact times are caused by the formation of a pronounced neck in the outgoing phase of the reaction.

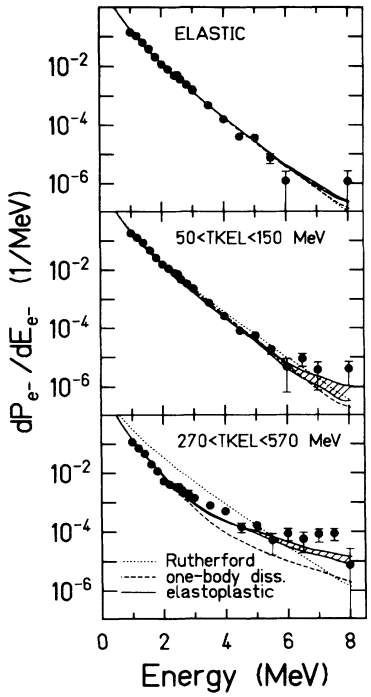

FIG. 1. Spectra of electron emission probability per collision of Pb+Pb at 12.0 MeV/nucleon incident energy. The curves are results of coupled-channel calculations based on the nuclear trajectories predicted by various reaction models (dotted: Rutherford trajectories; dashed: one-body dissipation model; hatched area in between the solid lines: elastoplastic model with $\alpha=6$–12 and $\beta=0.15$).

In Fig. 1 the results from calculations with trajectories obtained with the one-body dissipation model are shown by the dashed lines. Statistical fluctuations of the nuclear trajectories [8,18] can be neglected in our calculations as rather broad TKEL windows are used. The underestimation of the measured yield at high electron energies within this model evidences that there is not sufficient deceleration in the approach phase of the reaction. One could try to increase the stopping power by multiplying the microscopically calculated friction tensor by some factor. But this results in a shortening of the nuclear contact times, and hence leads to unacceptable discrepancies for the low-energy part of the δ-electron spectra. Of course, there are other friction models [18,19] which by a proper fit of the friction coefficients give faster deceleration and may even be consistent with the large contact times. However, already in the one-body dissipation model the deceleration is so fast (although still too slow compared to the experimental result of this paper) that the Markov assumption implied in this and all other friction models is questionable [20]. Indeed, the radial deceleration time $\tau_{\text{decel}} \approx 2\times10^{-22}$ s (cf. lower part of Fig. 2) while the thermal equilibration time $\tau_{\text{therm}} \approx (2\times10^{-22}\ \text{s MeV})/\varepsilon^*$, where ε^* denotes the excitation energy per nucleon [21]. Thus, $\tau_{\text{decel}} \lesssim \tau_{\text{therm}}$ during the

whole deceleration phase ($0 < \varepsilon^* \lesssim 1$ MeV) with the consequence that the dissipation process is essentially non-Markovian. By measuring high-energy δ electrons one is sensitive to time scales of the order of 10^{-22} s and hence memory effects can be investigated. Such memory effects have been extensively studied within the diabatic approach to dissipative collective nuclear motion [20,22]. This theory of dissipative diabatic dynamics (DDD) is closely related to the microscopic one-body dissipation model [20] which, therefore, is easily extended to include the memory effects as will be explained in the following.

In the one-body dissipation model the friction force for the macroscopic degrees of freedom q_j is given by $F_i^{\text{Markov}} = -\sum_j \gamma_{ij}(\mathbf{q})\dot{q}_j$, where $\gamma_{ij}(\mathbf{q})$ denotes the friction tensor. Guided by the importance of diabatic single-particle motion in dissipative heavy-ion collisions we have, for the shape degrees of freedom, replaced the Markovian friction force of the one-body dissipation model by a retarded friction force $\mathbf{F}$ as introduced in Ref. [20]. Its components are determined by the differential equation

$$\frac{dF_i}{dt} = -\frac{1}{\tau_{\text{intr}}(t)} F_i(t) - \sum_j C_{ij}(\mathbf{q})\dot{q}_j , \tag{2}$$

where $\tau_{\text{intr}}(t)$ and C_{ij} denote the intrinsic equilibration time and the stiffness tensor, respectively. In the limit of large τ_{intr}, such that the first term on the right-hand side can be neglected, the force depends explicitly neither on time nor on $\dot{q}$, and hence is conservative. In this case, the collective motion is elastic without any dissipation. In the opposite limit of small τ_{intr}, such that $F(t)$, C_{ij}, and $\dot{q}_j$ do not change considerably during time intervals of the order τ_{intr}, dF/dt can be neglected in Eq. (2), and hence the force becomes a pure friction force given by $-\sum_j C_{ij}\tau_{\text{intr}}\dot{q}_j$. For intermediate values of τ_{intr}, the system behaves like a damped oscillator with a frequency-dependent friction coefficient. The elastic response on fast deformations and the dissipative response on slow deformations is typical for elastoplastic materials like glass, glycerine, and "silly putty" (a plastic toy).

There is a close relationship between dissipative diabatic dynamics and the one-body dissipation model. Both approaches are based on the same microscopic picture which determines the collective motion from the distortion of the nucleonic Fermi distribution by the time-dependent shapes of the nuclear system. This coupling between intrinsic and shape degrees of freedom yields the stiffness tensor C_{ij} in the diabatic approach and it provides the friction tensor γ_{ij} in the one-body dissipation model via the additional assumption that the distortions in the nucleonic momentum distribution relax instantaneously. Indeed, for the quadrupole motion of a cube of matter the stiffness parameter C is related to the friction coefficient γ in the one-body dissipation model (wall formula) by [20]

$$C = \frac{24}{5} \times \frac{2}{9} \times \frac{\gamma}{\tau_{\text{s.p.}}} , \tag{3}$$

where $\tau_{\text{s.p.}}$ denotes the time of flight of a nucleon with Fermi velocity v_F through the cube. We assume the general validity of this relation in the form

$$C_{ij}(q) = \alpha\gamma_{ij}(q)/\tau_{\text{s.p.}} , \tag{4}$$

with $\tau_{\text{s.p.}} = 2R_0/v_F$ and $R_0 = 1.2(A_1+A_2)^{1/3}$ fm the radius of the compound nucleus. Here, a parameter α is introduced to correct for shortcomings of the simple cube model with respect to realistic shapes, single-particle potentials, and effective nucleon masses m_{eff}. According to the microscopic expression [20,23], the stiffness tensor C_{ij} is proportional to $m_{\text{eff}}^{-5/2}$ and to the level density which experimentally is twice its Fermi-gas value. Since $\gamma_{ij}/\tau_{\text{s.p.}}$ is reduced from the Fermi-gas model with $m_{\text{eff}} = m_{\text{nucleon}}$, we expect $\alpha \approx 2m_{\text{eff}}^{-5/2}$, which yields $\alpha \approx 5$ for a realistic value of $m_{\text{eff}} = 0.7m_{\text{nucleon}}$. Furthermore, compression is not allowed in the collective model, and hence we expect even larger values (larger by roughly a factor of 2 corresponding to $\alpha \approx 10$) for the stiffness coefficient to be effective in the approach phase.

For the intrinsic equilibration rate τ_{intr}^{-1} we consider three major contributions,

$$\tau_{\text{intr}}^{-1} = \tau_2^{-1} + \tau_x^{-1} + \tau_a^{-1} . \tag{5}$$

The first term results from two-body collisions and is estimated by Bertsch [21] as $\tau_2^{-1} = \varepsilon^*/t^*$ with ε^* denoting the excitation energy per particle and $t^* = 2\times 10^{-22}$ MeV s. The rate τ_x^{-1} is associated with the decay of diabatic states due to quasicrossings. This rate is given in Ref. [24] as $2\pi|H'|^2/\hbar\delta_x$ with H' the mean coupling matrix element between the diabatic states and δ_x the mean distance in energy between quasicrossings along a diabatic level. For realistic values $\delta_x \approx 2$ MeV and $H' \approx 0.5$ MeV we obtain $\tau_x \approx 0.8\times 10^{-21}$ s. The last term accounts for the decay of diabatic states due to couplings proportional to the acceleration $\ddot{q}$. From the "golden rule" and the microscopic expression [25] for the coupling Hamiltonian we write $\tau_a^{-1} = \beta\ddot{q}^2(10^{-21}\text{ s})^3\text{ fm}^{-2}$ with β estimated to 0.1 using a mean absolute value of $0.2R_0|\dot{q}|$ for the single-particle matrix element of the velocity potential.

In the new diabatic one-body dissipation model the parameters α and β, estimated above, influence the stopping power and the nuclear interaction times almost independently. As a result of the retardation of the frictional force, a large repulsive potential (proportional to α) is built up in the approach phase which leads to a fast deceleration. As a result of this fast deceleration, the decay rate of the diabatic potential is mainly determined by τ_a^{-1}, and hence is sensitive to the parameter β. A fast enough decay is decisive for a long contact time, because it prevents the nuclei from bouncing back elastically. The hatched areas in between the solid lines in Fig. 1 are the theoretical predictions obtained with the elastoplastic model using $\beta = 0.15$ and α values between 6 and 12. Values of α larger than 12 do not change the result

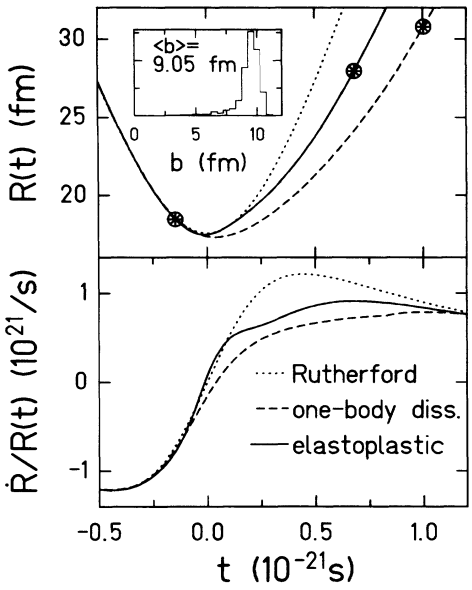

FIG. 2. Nuclear trajectories in terms of twice the root-mean-square radius, $R(t)$, and $\dot{R}/R(t)$ as a function of time for the highest TKEL window. The spoke-wheel symbols denote the instants of touching and separating shapes [15].

significantly. At high TKEL values the intrinsic equilibration rate is mainly determined by two-body collisions, leading to a weak sensitivity on the parameter β. Details of the calculations are the subject of a forthcoming paper (see also Ref. [26]). There it will be shown that the diabatic extension also describes the experimental correlation between scattering angles and TKEL values better than the original one-body dissipation model.

Figure 2 illustrates the nuclear trajectories for the highest TKEL window. They have been calculated using the mean impact parameter deduced from the impact parameter distribution shown in the inset. In contradistinction to the smooth $\dot{R}/R(t)$ curves of the Rutherford and the one-body dissipation trajectories the elastoplastic trajectory shows a faster deceleration connected with additional weak oscillations, leading to the increased yield of high-energy δ electrons seen in Fig. 1.

In summary, studying the Pb+Pb collisions at 12.0 MeV/nucleon a very fast radial deceleration is deduced from the yield of the high-energy part of the δ-electron spectra. It is much stronger than predicted by the one-body dissipation model [15]. The extension of this model by including diabatic effects according to Ref. [20] allows us to account for the two aspects of the experimental data, the fast stopping and the long contact times. This strongly supports the existence of an elastoplastic behavior of nuclear matter in dissipative heavy-ion collisions.

We would like to thank S. Graf and Th. de Reus from the University of Frankfurt for their help in running the coupled-channel code. The construction of dedicated electronic units by J. Foh and the electronic workshop and the production of the large-area silicon counter by W. Patzner, both of the Institut für Kernphysik, Darmstadt, as well as the preparation of the targets by H. Folger and the GSI target laboratory are gratefully acknowledged. This work is supported by the Bundesministerium für Forschung und Technologie under Contract No. 06DA453 and by the Gesellschaft für Schwerionenforschung, Darmstadt.

[1] G. Soff, J. Reinhardt, B. Müller, and W. Greiner, Phys. Rev. Lett. **43**, 1981 (1979).
[2] E. Kankeleit, Nukleonika **25**, 253 (1980).
[3] E. Kankeleit, in *International Advanced Courses on Physics of Strong Fields*, edited by W. Greiner (Plenum, New York, 1987).
[4] U. Müller, G. Soff, J. Reinhardt, T. de Reus, B. Müller, and W. Greiner, Phys. Rev. C **30**, 1199 (1984).
[5] R. Krieg *et al.*, Phys. Rev. C **34**, 562 (1986).
[6] M. Krämer *et al.*, Phys. Lett. B **201**, 215 (1988).
[7] J. Stroth *et al.*, Ric. Sci. Educ. Permanente, Suppl. **63**, 659 (1988) (*Proceedings of the XXVI International Winter Meeting on Nuclear Physics, Bormio, 1988*, edited by I. Iori).
[8] M. Krämer *et al.*, Phys. Rev. C **40**, 1662 (1989).
[9] Th. de Reus, J. Reinhardt, B. Müller, U. Müller, G. Soff, and W. Greiner, Z. Phys. A **321**, 589 (1985).
[10] E. Kankeleit *et al.*, Nucl. Instrum. Methods Phys. Res., Sect. A **234**, 81 (1985).
[11] M. Rhein and Ch. Müntz, GSI Annual Report, 1989 (unpublished), p. 293.
[12] R. S. Hager, E. C. Seltzer, and V. F. Trusov, in *Atomic and Nuclear Data Reprints, Internal Conversion Coefficients*, edited by K. Way (Academic, New York, 1973).
[13] P. Schlüter, G. Soff, and W. Greiner, Phys. Rep. **75**, 327 (1981).
[14] Th. de Reus *et al.*, Phys. Rev. C **40**, 752 (1989).
[15] H. Feldmeier, Rep. Prog. Phys. **50**, 915 (1987).
[16] W. U. Schröder and J. R. Huizenga, in *Treatise on Heavy-Ion Science*, edited by D. A. Bromley (Plenum, New York, 1984), Vol. 2, and references therein; J. Randrup, Nucl. Phys. **A327**, 490 (1979).
[17] J. Blocki *et al.*, Ann. Phys. (N.Y.) **113**, 330 (1978).
[18] P. Fröbrich and J. Stroth, Phys. Rev. Lett. **64**, 629 (1990).
[19] R. Schmidt, V. D. Toneev, and G. Wolschin, Nucl. Phys. **A311**, 247 (1978).
[20] W. Nörenberg, Phys. Lett. **104B**, 107 (1981); in *Heavy Ion Reaction Theory*, edited by W. Q. Shen, J. Y. Li, and L. X. Ge (World Scientific, Singapore, 1989), and in *New Vistas in Nuclear Dynamics*, edited by P. J. Brussaard and J. H. Koch (Plenum, New York, 1986).
[21] G. F. Bertsch, Z. Phys. A **289**, 103 (1987).
[22] P. Rozmej and W. Nörenberg, Phys. Lett. **117B**, 278 (1986).
[23] A. Lukasiak and W. Nörenberg, Z. Phys. A **326**, 79 (1987).
[24] W. Cassing and W. Nörenberg, Nucl. Phys. **A433**, 467 (1985).
[25] A. Lukasiak, W. Cassing, and W. Nörenberg, Nucl. Phys. **A426**, 181 (1984).
[26] M. D. Rhein, Ph.D. thesis, Institut für Kernphysik, TH-Darmstadt, 1991 (unpublished).